Argonne NATIONAL LABORATORY

ANL/CFCT-20/30

Selection and Characterization of Surrogate Material for Developing Zr Barrier Coatings for Uranium Nitride Particles

Chemical and Fuel Cycle Technologies Division

ANL/CFCT-20/30

Selection and Characterization of Surrogate Material for Developing Zr Barrier Coatings for Uranium Nitride Particles

prepared by
Sumit Bhattacharya[1], Rachel Seibert[2], Andrew Nelson[2], Heather Connaway[1], Abdellatif Yacout[1]

1) Argonne National Laboratory
2) Oak Ridge National Laboratory

June 2021

(This page left intentionally blank)

Abstract

In support of $UC_{1-x}N_x$ fuel kernels (~ 800 micrometer diameter) development work ongoing at Oak Ridge national laboratory (ORNL), where the fuel kernels will be embedded inside a possible zirconium based matrix, Argonne National Laboratory (ANL) is contributing to help develop a robust metal diffusion barrier coating. Zirconium nitride (ZrN) and Zirconium oxide (ZrO2) were selected as possible diffusion barrier candidates, and the atomic layer deposition (ALD) has been chosen as a candidate technology to deposit the film. Development of such a barrier coating with the ALD process entails significant number of trials to study relevant parameters. Therefore, to prevent needless wastage, instead of coating directly over fuel kernels, a surrogate candidate with similar dimensions and physical properties were been selected and coated to develop the diffusion barrier coating.

Table of Contents

1 Introduction

In support of $UC_{1-x}N_x$ fuel kernels (~ 800 micrometer diameter) development work ongoing at Oak Ridge national laboratory (ORNL), where the fuel kernels will be embedded inside a possible zirconium based matrix, Argonne National Laboratory (ANL) is contributing to help develop a robust metal diffusion barrier coating. One micrometer thick Zirconium nitride (ZrN) and Zirconium oxide (ZrO_2) have been selected as possible diffusion barrier candidates to thwart high temperature Zr mixing with the $UC_{1-x}N_x$ fuel kernels, while atomic layer deposition (ALD) has been chosen as a candidate technology to deposit the film. Development of such a barrier coating with the ALD process entails a significant number of trials to study parameters such as growth performance and mechanical/thermal stability of the coating, which necessitates quick characterization of the coated substrates.

Therefore, instead of coating directly over the $UC_{1-x}N_x$ fuel kernels of interest, to prevent needless waste surrogate candidate with similar dimensions and physical properties (in this case, thermal expansion properties, thermal conductivity and most importantly surface chemistry) were selected and coated to develop the diffusion barrier coating. Spherical particles of WC-Co cemented carbide with diameter ~ 800 micrometers are found to be an ideal surrogate to test ALD ZrN and ZrO_2 coating mechanical/thermal stability, when exposed to different temperatures.

Based on the characterization results from the coated surrogate material, it was concluded (a) no thicker than 100 nm of ALD ZrN can be applied as thicker coating suffers from residual stress related cracking and eventual spallation, (b) whereas with ALD ZrO_2 the final target thickness of one micrometer is achieved without issues. To verify the observations made from the surrogate, similar deposition studies are repeated over actual $UC_{1-x}N_x$ fuel kernels and the coated fuel kernels displayed analogous results.

Therefore, in this report, the detailed ALD development for both ZrN and ZrO_2 coatings and corresponding characterizations performed over surrogate particles which helped determine the final coating condition over $UC_{1-x}N_x$ fuel kernels are presented.

2 Experimental Procedures

2.1 UC1-xNx fuel kernels

$UC_{1-x}N_x$ microspheres were fabricated via solution-gelation (sol-gel) and conversion, performed at ORNL. The resulting kernels had an average diameter of 810 μm and a density of 13.60g/cm^3 (94.89% TD) [1]. No specific details regarding the thermal expansion coefficient and net carbon residual amount present in the $UC_{1-x}N_x$ fuel kernels was provided for this study or is currently available in the published literature. Figure 1 (a, b) shows the typical morphology and surface condition of the as received fuel kernels from ORNL. The kernel presents a rough texture, with observable surface oxidation (Figure 1(b)) most likely due to exposure in the ambient atmosphere during transport and analysis. Detailed surface compositions can be found in Table 1.

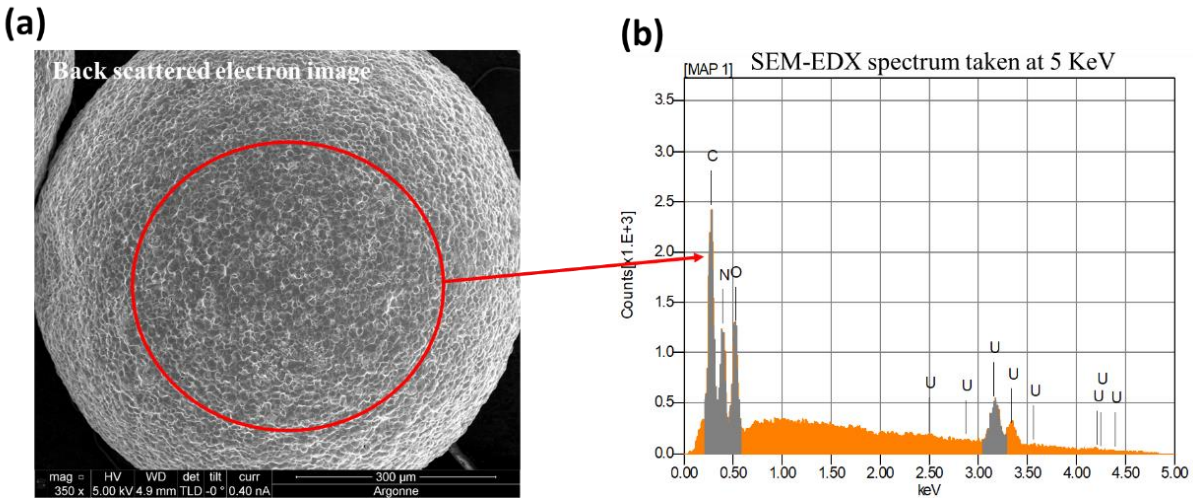

Figure 1: (a) UC1-xNx fuel kernels as received from ORNL; (b) EDS spectrum performed over the kernel surface (marked by red circle).

Table 1: $UC_{1-x}N_x$ fuel kernels surface composition

Elements	mass%	Atom%
C	1.65	18.88
N	1.59	15.66
O	1.17	10.10
U	95.59	55.36

2.2 Surrogate Material

ORNL has identified ZrO_2 or Yttria-stabilized ZrO_2 (YTZ) as a surrogate candidate to produce tri-isotropic (TRISO) coated fuel particles for $UC_{1-x}N_x$ fuel kernels [2]. ZrO_2 spheres will not be an ideal candidates to use for quantifying ALD ZrN and ZrO_2 coating physical properties and stabilities, due to similar elemental constituents especially for ALD zirconium oxide coating. Such a surrogate will not only provide a much better nucleation surface for ALD coating because of similar surface chemistry [3], but will also make coating characterization incredibly challenging, especially for ALD ZrO_2. One of the relevant experiments is to examine the coating stability at high temperature steam/air (deposited ALD coating is also expected to provide oxidation barrier properties in case of any failure scenarios) using a thermogravimetric analyzer (TGA). So using a surrogate which is already completely oxidized would make measurements challenging. Thus, it is important when selecting a material to identify one which not only presents similar physical properties when compared to $UC_{1-x}N_x$ fuel kernels, but also displays similar oxidation behavior such that at high temperature during TGA analysis if the coating fails, immediate changes in the coated surrogate weight is identified.

There are very few materials that exhibit oxidation behavior like the uranium nitride system. Most of the common nitride or carbide (e.g. Si, Ti, Al, Zr, Cr based nitrides and carbides) ceramics display remarkably high oxidation resistance against air and steam. From the literature, the best two metal-based nitrides and carbides that match the requirements for an ideal surrogate are Mo and W. Carbides and nitrides for both Mo and W seems to be highly reactive and form volatile compounds (>600ºC) when exposed to high temperature at ambient conditions [4, 5, 6]. For the

specific cases of Molybdenum nitride/carbide and Tungsten nitride, unfortunately spherical particles of the required dimensions of these chemistries are not commercially available. Whereas for the case of WC, due to its extremely high hardness and wear resistant properties, WC mixed with small amount of Co as a binder is utilized as a grinding, milling and cutting medium. Thus, spheres of ~ 800 micrometer of this material are readily available and is an ideal surrogate for $UC_{1-x}N_x$ fuel kernels.

The ~ 800-micron WC-Co cemented carbide spheres were purchased from Fritsch, for performing ball milling. The material properties of this material can be found in Table 2 [7]. Figure 2 (a, b) shows the typical morphology and surface condition of the as received WC-Co spheres. Detailed surface compositions can be found in Table 3.

Table 2: General specifications of the as received WC-Co surrogate spheres

Material	Tungsten carbide - WC
Elements	Share %
Tungsten carbide – WC	88
Cobalt – Co	12
Physical and mechanical properties	
Density	14.3 g/cm³
Hardness	89.7 HRA
Thermal expansion coefficient at 1000 °C	~10 x 10^{-6} /K

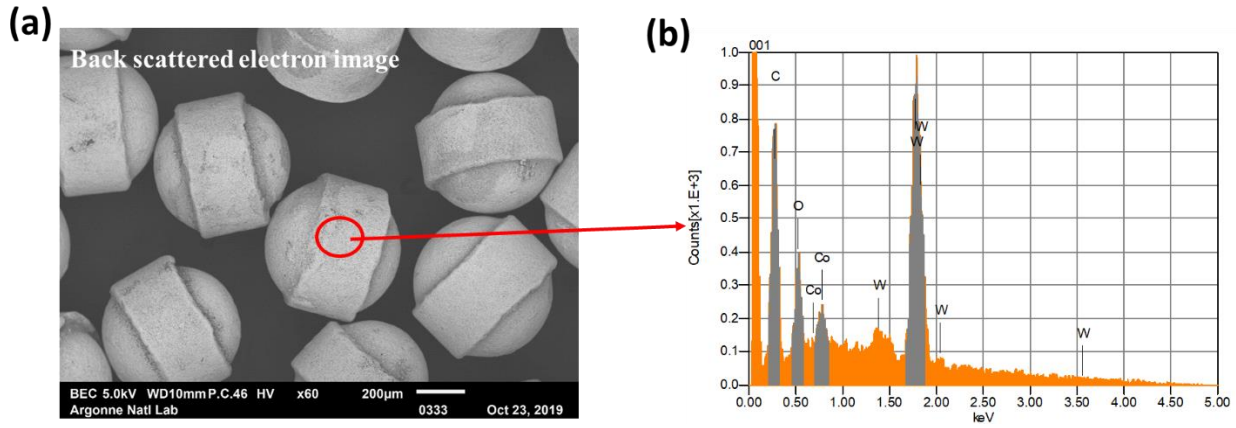

Figure 2: (a) ~800 micrometer spheres of WC-Co cemented carbides; (b) EDS spectrum performed over WC-Co (marked by red circle).

Table 3: WC-Co cemented carbide sphere surface composition

Elements	mass%	Atom%
C	8.16	49.15
O	2.71	12.25
Co	4.22	5.18
W	84.91	33.41

2.3 ALD Coating

2.3.1 ALD ZrN Coating Process

Before depositing ZrN, the WC-Co cemented carbide spheres were preheated to 200 °C and maintained for 2 to 3 hours in order to remove any volatile material present on the surface. Deposition of ALD ZrN thin films over WC-Co cemented carbide spheres was performed using Tetrakis(dimethylamido)zirconium (IV) (TDMAZr) and ammonia (NH_3) as the alternating precursor [8]. Both TDMAZr and NH_3 are electronic grade procured from Sigma-Aldrich and Airgas, respectively. For ZrN ALD film growth, the substrate was heated to a temperature of ~220 °C followed by a consecutive exposure of TDMAZr and NH_3. This temperature has been selected based on previous work, whose details can be found in reference [9]. In between pulses purging was performed with nitrogen (N_2) gas to remove residual reactants and reaction products.

The ALD ZrN sequence can be defined as an A-B cycle, where both A and B represent individual reaction half cycle happening over the surface. The timing for these sequences is (a) TDMAZr exposure time (~1.5 s) (b) N_2 purging time (10 s) (c) NH_3 exposure time (0.1 s) and finally (d) N_2 purging time (10 s). The repetition of the A-B cycles results in a ZrN ALD film with a growth rate of ~1.05 Å for each cycle. Based upon previous experience of ALD ZrN coating over U-Mo dispersion fuel powder, where significant spalling was observed after deposition of one micrometer coating, this deposition is carried in stages – after every 1000 cycles or ~ 105 nm, samples of WC-Co were taken out for surface characterization. The ALD ZrN surface reaction can be described by Eqs. (1) and (2) (Note. asterisks indicate the surface species in all equations) and the deposition of ZrN is realized as a combination of transamination exchange and amine elimination reactions [10].

$$\text{(A-cycle) } 2NH^* + Zr(N(CH_3)_2)_4 = N_2Zr(N(CH_3)_2)_2)^* + 2HN(CH_3)_2 \quad (1)$$

$$\text{(B-cycle) } N_2Zr(N(CH_3)_2)_2)^* + 4/3NH_3 = N_2ZrNH_2^* + 2HN(CH_3)_2 + 1/6N_2 \quad (2)$$

2.3.2 ALD ZrO_2 Coating Process

Deposition of ALD ZrO_2 thin films over WC-Co cemented carbide spheres was performed using TDMAZr and distilled water (H_2O) were used as reactants to develop the oxide phase. The same batch of TDMAZr was used for this coating, while in-house distilled form of water was used. The two sequential, self-limiting reactions for ZrO_2 ALD are described by equation (3) and (4) [11].

$$\text{(A-cycle) } Zr\text{-}(OH)_2^* + Zr(N(CH_3)_2)_4 = Zr\text{-}(O)_2\,Zr(N(CH_3)_2)_2)^* + 2HN(CH_3)_2 \quad (3)$$

$$\text{(B-cycle) } Zr\text{-}(O)_2\,Zr(N(CH_3)_2)_2)^* + 2H_2O = Zr\text{-}(OH)_2^* + 2HN(CH_3)_2 \quad (4)$$

For ZrO_2 ALD growth, the heated WC-Co cemented carbide spheres were first exposed to TDMAZr, followed by a N_2 purge to remove the residual reactants and reaction products. The

substrate was subsequently exposed to water followed by a second N_2 purging process. This sequence is similar to that of ALD ZrN process. The timing for this sequence is (a) TDMAZr exposure time (1.0 seconds), (b) N_2 purging time (10 seconds), (c) water exposure time (0.25 second), and finally (d) second N_2 purging time (10 seconds). The ALD ZrO_2 has a growth rate of ~1.1 Å per cycle at 220 ^oC and in total 9100 cycles of TDMAZr and H_2O are pulsed, to develop an ~1000 nm thick coating. The resultant ALD ZrO_2 film is nano crystalline in nature [12].

2.4 ALD Deposition Device and Characterization Technique

The ALD device used to execute this work is described here. The ALD device at ANL is a commercial wafer coating ALD system procured from Ultratech Company, which has been modified to accommodate diverse sample shape and size. This was achieved with a custom-built lid, designed and constructed at ANL, dedicated for deposition of thin films over powder-based substrates, and serving as a prototype for future large-scale coating. The modified ALD setup is assembled inside a custom-built glove box from M-Braun, in order to maintain a low-oxygen (<0.2 ppm) environment for the air sensitive ALD coating and substrate handling. A hollow rotating drum design has been used in this case, to contain the powder while allowing the ALD precursors to come through, react and finally exhaust out via its two openings at both ends. The hollow drum is rotated with a magnetic motor drive, which prevents powder agglomeration, while allowing uniform coating of the powders.

The microstructure of the coated and uncoated WC-Co cemented carbide spheres and $UC_{1-x}N_x$ fuel kernels were characterized by scanning electron microscope (SEM), model JSM-IT100 In Touch Scope and detailed cross sections of the coated spheres were characterized with focused ion beam (FIB), model FEI HELIOS Nano Lab 600 Dual Beam FIB/SEM.

3 Results

The subsections below discuss the results of the coating tests, presented for two different thicknesses of ZrN coating and for ZrO_2 coating.

3.1 WC-Co cemented carbides coated with ALD ZrN

3.1.1 Coating Thickness 100 nm ZrN

After completion of 1000 cycles, the ALD ZrN coating process was halted to collect samples of coated surrogate spheres for characterization. The coated powders were cooled to room temperature before they were taken out of the ALD chamber. Figure 3 (a) displays the characteristic surface condition of the deposited ZrN coating. No observable cracks or spallation is observed. From the EDS spectrum (Figure 3 (b)) collected over the coated surrogate surface (identified by the red circle), other than small amount of oxygen and carbon (Table 4), the coating is mostly ZrN. The carbon residue can originate from the ALD process itself, where during each monolayer formation over the substrate surface, sometimes the carbon ligands attached to the TDMAZr precursor may stay behind instead of leaving the system as reaction product [13]. In regard to the observed oxygen, it can come from the native oxide formation over the ZrN surface when exposed to the ambient atmosphere.

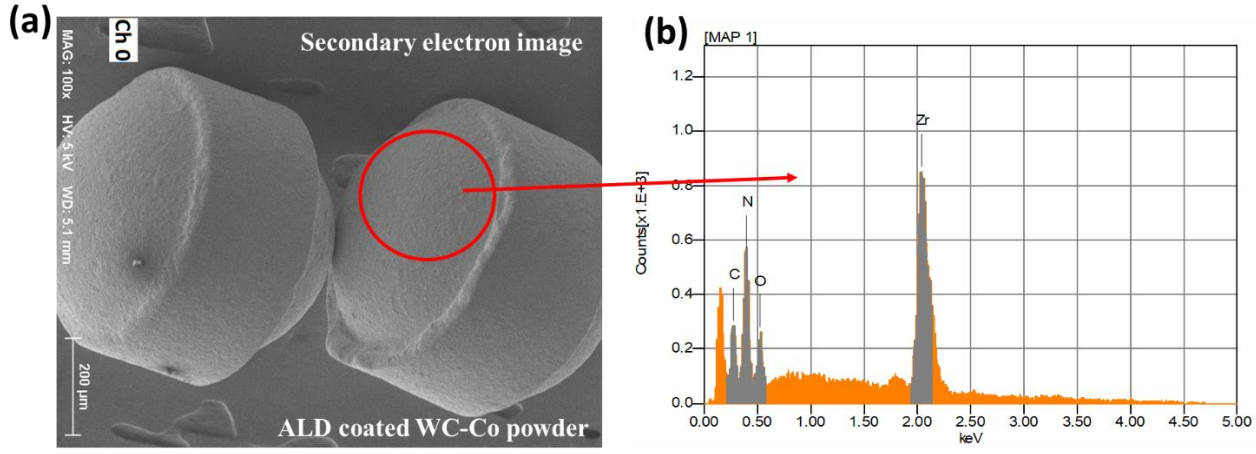

Figure 3: (a) ~800 micrometer spheres of WC-Co cemented carbides, after 1000 cycles of ALD ZrN deposition; (b) EDS spectrum (5 KeV) performed over coated WC-Co (marked by red circle).

Table 4: WC-Co cemented carbide sphere surface composition after coated with 1000 cycles of ALD ZrN

Elements	Mass%	Atom%
C	3.13	11.53
N	13.60	42.91
O	2.29	6.32
Zr	80.98	39.24

In order to measure the exact ZrN coating thickness achieved over the WC-Co carbide surrogates, FIB operation was done, where in total 5 coated surrogate particles were dug to expose a cross sectional region of ~ 40-micron x 30-micron. In each of those 5 dug particles, 10 different cross-sectional approximate measurements of the deposited coating were recorded. The mean thickness based on the measurements was ~ 110 nm (+/- 5 nm) of ALD ZrN after 1000 cycles of deposition. Figure 4 (a) is an example of one such segmented area performed to expose the coating cross section (note, image is taken at 52° tilt from the electron detector using a FIB device). From Figure 4 (a), a continuous bonding between the ALD ZrN and surrogate is also observed. An EDS line scan (Figure 4 (b)) was performed along the cross section (ALD ZrN coating surrogate interface) to confirm the precise interface that is generally expected from a ALD deposition process.

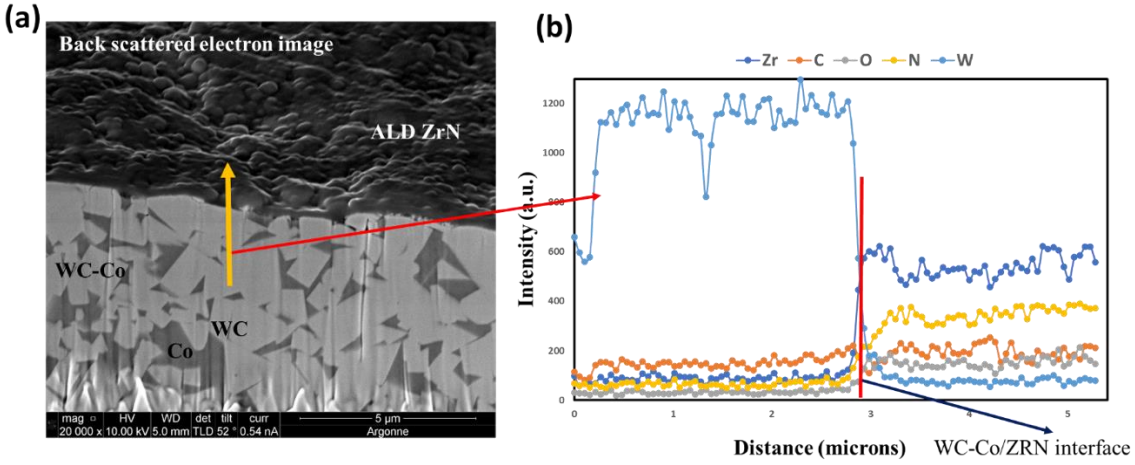

Figure 4: (a) FIB cross section (image collected at 52° tilt from the electron detector) of the ALD ZrN coating. From 10-point measurements, ~ 110 nm thickness was measured; The bright rectangular regions seen at the cross section is WC and the dark matrix is Co, (b) EDS Line scan (KeV) performed at the cross section of the coated WC-Co particle, the red

line over the line scan plot indicates interface between ZrN and WC-Co cemented carbide sphere.

3.1.2 Coating Thickneess 200 nm ZrN:

After completion of another 1000 cycles over the already-coated surrogates with 100 nm ALD-applied ZrN, the deposition was halted to collect samples of the more heavily coated surrogate spheres for further characterization. The coated powders were cooled to room temperature before they were taken out of the ALD chamber. Figure 5 (a) displays the characteristic surface condition of the deposited ZrN coating. Immediately large observable cracks or spallation is observed, especially in the curved region of the sphere present across the equator. To verify that the crack has not resulted due to thermal mismatch stresses present at the equatorial region of the surrogate spheres, the coating over the spherical surface was also studied. The surface cracks present all over the coating are directly observed at higher magnification (Fig. 5(b)). This issue is similar to what has been previously observed while depositing ALD ZrN directly over U-Mo dispersion fuel particles [8]. From the EDS spectrum (Figure 5 (c)) collected over the coated surrogate surface (from non-spalled region), again other than a small amount of oxygen and carbon (Table 4), the coating chemistry is mostly ZrN. The carbon residue in this case is slightly higher than the 100 nm ALD ZrN coating. This can be again explained from the description in previous section and now more carbon has accumulated from unreacted ligands from TDMAZr precursor. [13]. The oxygen content can be also explained with the same description presented in previous section.

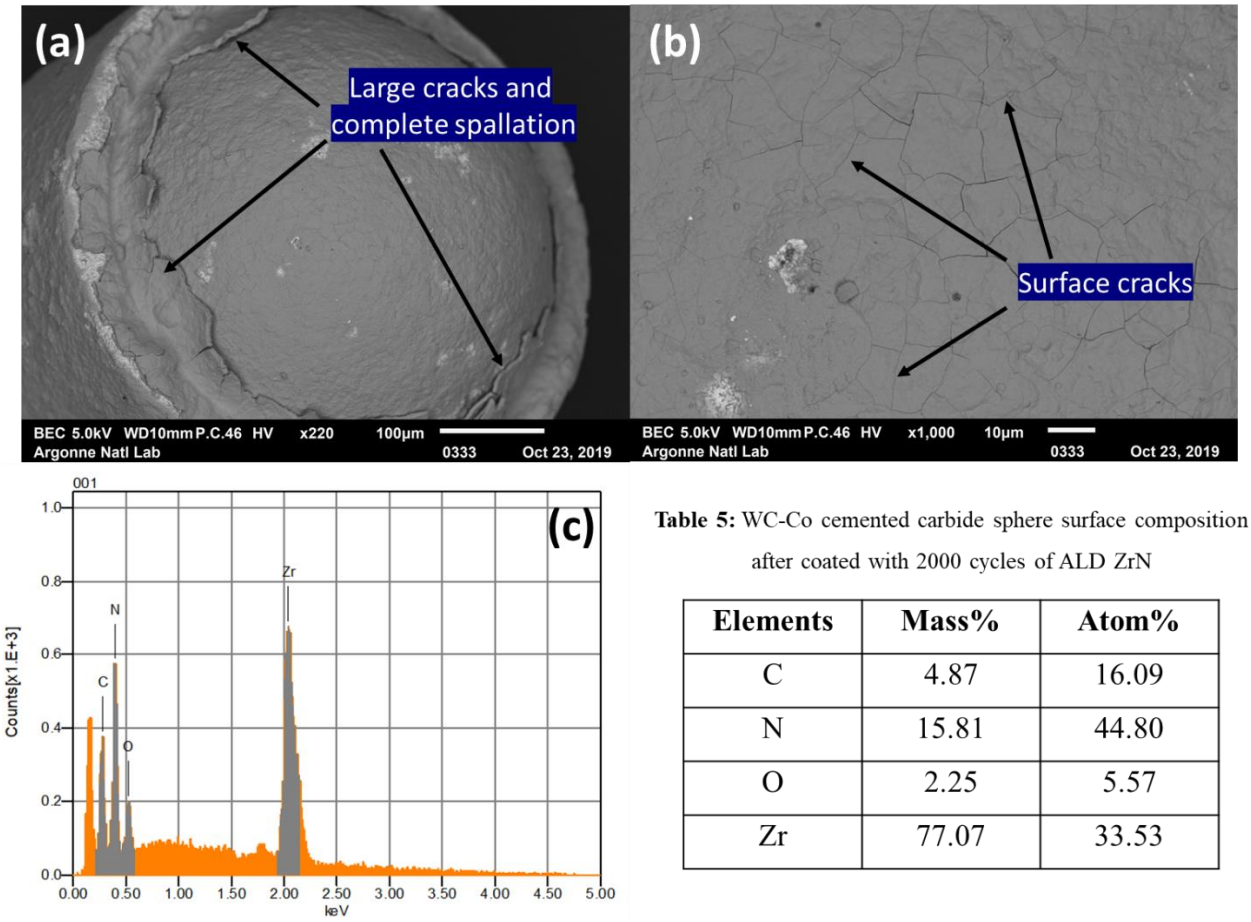

Table 5: WC-Co cemented carbide sphere surface composition after coated with 2000 cycles of ALD ZrN

Elements	Mass%	Atom%
C	4.87	16.09
N	15.81	44.80
O	2.25	5.57
Zr	77.07	33.53

Figure 5: (a) ~800 micrometer spheres of WC-Co cemented carbides, after 2000 cycles of ALD ZrN deposition; large cracks and significant spallation were observed (b) The regions of the ALD ZrN coating which did not yet showed signs of large cracks, also showed small surface cracks when viewed at a higher magnification (c) EDS spectrum (5 KeV) performed over 2000 cycles ALD ZrN coated WC-Co where the coating has not yet spalled off. Table 5 presents the surface composition of the deposited ALD ZrN coating measured in non-spalled region of the sphere.

To verify the spalled regions seen over the surrogate surface, EDS mapping was performed. Figure 6 (a) is showing the region over which the mapping had been performed. Figure 6 (b) shows W distribution and Fig. 6 (c) Zr distribution over the coated sphere. It is evident that W can be observed even with just 5 KeV of electron beam energy, which was not possible for 100 nm ZrN coating, therefore it can be concluded large sections of the ALD ZrN coating has spalled off from the surface. Figure 6 (d) and Table 6 confirms the observation as identified from the EDS spectrum and elemental composition developed from the studied region.

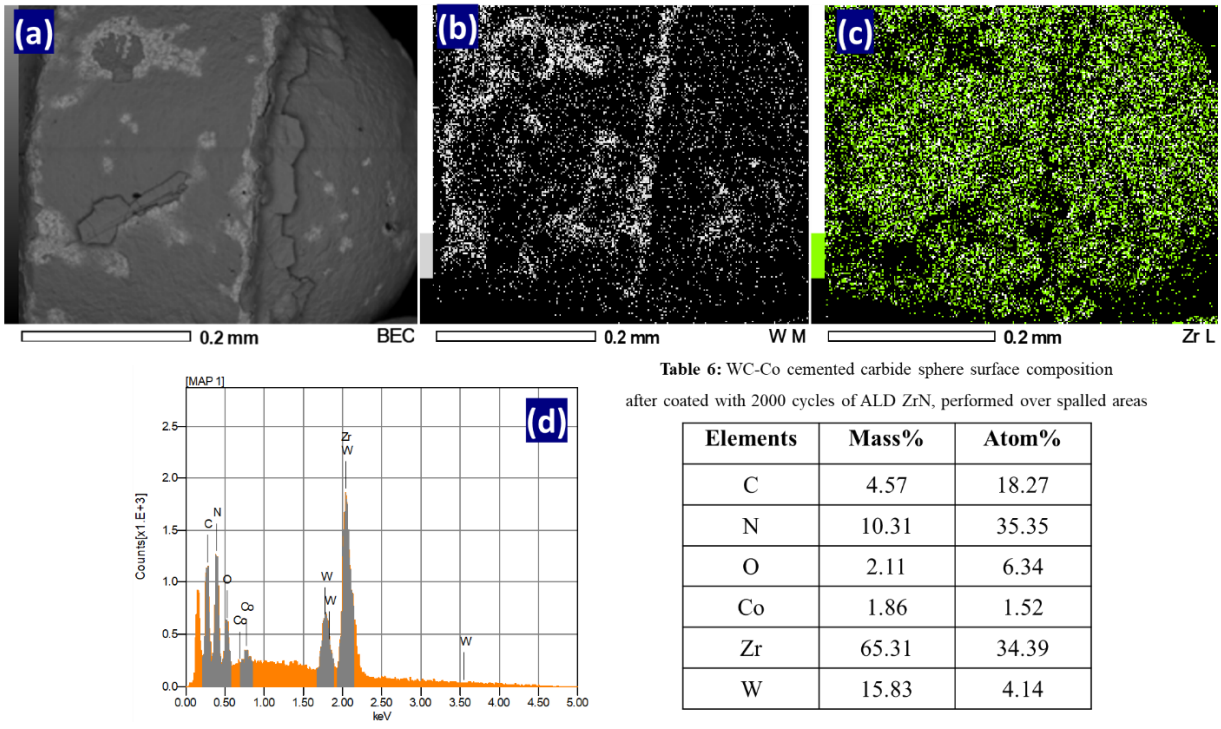

Table 6: WC-Co cemented carbide sphere surface composition after coated with 2000 cycles of ALD ZrN, performed over spalled areas

Elements	Mass%	Atom%
C	4.57	18.27
N	10.31	35.35
O	2.11	6.34
Co	1.86	1.52
Zr	65.31	34.39
W	15.83	4.14

Figure 6: (a) SEM image of the area selected over the surrogate sphere coated with 2000 cycles of ALD ZrN, where the EDS mapping had been performed. (b) EDS mapping for W, (c) EDS mapping for Zr, (d) EDS spectrum (5 KeV) from the mapped region. Table 6: Surface elemental composition of the mapped region.

3.2 WC-Co cemented carbides coated with ALD ZrO_2:

After completion of 9100 cycles, the ALD ZrO_2 coating process was halted, to collect samples of coated surrogate spheres for characterization. The coated powders were cooled to room temperature before they were taken out of the ALD chamber. Figure 7 (a) displays the characteristic surface condition of the deposited ZrO_2 coating. No observable cracks or spallation is observed. In order to measure the exact ZrO_2 coating thickness achieved over the WC-Co carbide surrogates, FIB operation was done, where in total 5 coated surrogate particles were dug to expose a cross sectional region of ~ 40-micron x 30-micron. In each of those 5 dug particles, 10 different cross-sectional approximate measurements of the deposited coating were recorded. The mean thickness based on this measurement was ~ 1060 nm (+/- 25 nm) of ALD ZrO_2 after 9100 cycles of deposition. Figure 7 (b) is an example of one such segmented area performed to expose the coating cross section. From Figure 7 (b), a continuous bonding between the ALD ZrO_2 and

surrogate is also observed. From the EDS spectrum (Figure 7 (c)) collected over the coated surrogate surface, the samples display a stoichiometric coating where other than the constituent elements of the coating no residual material is observed. The elemental composition measured (Table 7) confirms that the deposited coating is indeed ZrO_2.

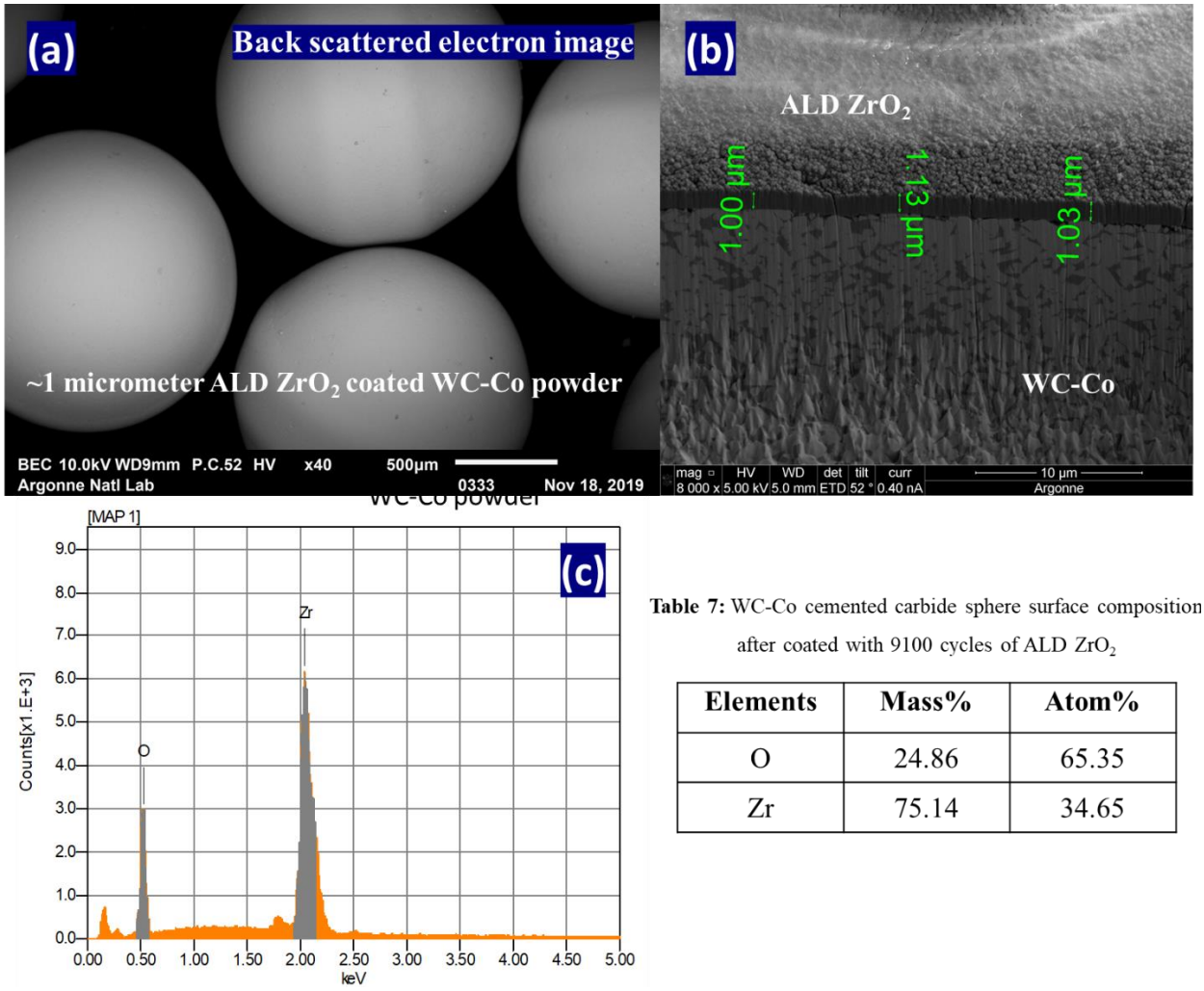

Table 7: WC-Co cemented carbide sphere surface composition after coated with 9100 cycles of ALD ZrO_2

Elements	Mass%	Atom%
O	24.86	65.35
Zr	75.14	34.65

Figure 7: (a) ~800 micrometer spheres of WC-Co cemented carbides, after 9100 cycles of ALD ZrO_2 deposition; (b) FIB cross section of the ALD ZrO_2 coating, based upon 10-point measurements~ 1060 nm (+/- 25 nm) of thickness was measured; The bright rectangular regions seen at the cross section is WC and the dark matrix is Co; (c) EDS spectrum performed over coated WC-Co, showing only Zr and O_2. Table 7: Elemental composition of the coating.

4 Discussion

4.1 ALD ZrO_2 properties

Detailed ALD ZrN microstructural and physical characteristics can be found in previously-published work [8, 12]. A discussion of ALD ZrO_2 properties is provided here.

4.1.1 Microstructure and phase identification:

For ALD ZrO_2 coating to be employed as a successful diffusion barrier coating against both Zr and O_2, it is vital to understand the type of microstructure that is developed after 9100 cycles of deposition performed at 220°C, as it will determine the diffusion paths of the unwanted materials through the coating. It is also important to determine the crystal structure of the deposited coating as ZrO_2 has three different structures. Out of these, (case a) cubic is most desirable due to its lower volume change at high temperature when it transforms into a monoclinic structure, but (case b), if the metastable tetragonal phase can be formed at low temperature and can remain stabilized throughout the whole application temperature range, it is also desirable.

To study the grain structure evolution and overall microstructure of the ALD ZrO_2 coating, a small TEM foil was prepared. Figure 8 (a) is a bright field TEM image of a cross sectional coating sample. From the TEM image it is confirmed that the deposited coating has a crystalline structure, where the grains are more equiaxial with ~ 20-25 nm size distribution. Figure 8 (b), presents the selected area diffraction pattern (SADP) obtained over the coating region. From the pattern analysis, it is evident that the ALD ZrO_2 seems to have a tetragonal crystal structure instead of a monoclinic structure which has been previously reported for similar ALD chemistry [14]. This metastable structure is generally formed at high temperature, but instances where such structures are seen at low temperatures are generally due to application of stress or due to presence of a second phase in the matrix. Direct deposition of such a crystal structure may be a result due to the ALD process itself or may be due to the residual stresses that accumulate during growth cycles. All in all, this is advantageous for the targeted application as the coating structure is already matched for high temperature application, and no phase transformation will occur which in turn increase the longevity of the coating by preventing unnecessary swelling. More detailed studies

are required, to invstigate if this coating can maintain its crystalline nature or if some kind of stabilizer is necessary. All these tests need to be performed at high temperature.

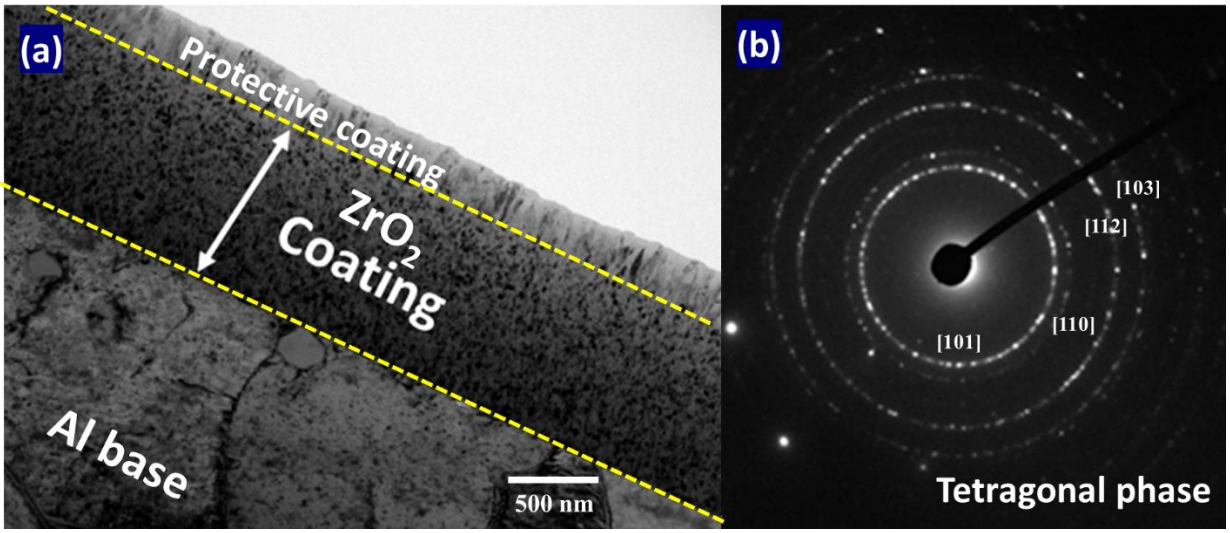

Figure 8: (a) TEM bright field of the ~1000 nm ALD ZrO_2 coating cross section. (b) SADP from the coating region, identified as a tetragonal crystal structure.

4.1.2 ALD ZrO_2 density estimation

Density of the applied barrier coating, in this case ALD ZrO_2, needs to be as close to the theoretical density as possible to be effective diffusion barrier. This is because a low-density coating will have more internal defects (e.g. point defects, residual contaminations), which will result in poorer performance. So, a preliminary estimation of the barrier coating density is necessary. Methods such as X-ray reflectivity (XRR) and quartz crystal microbalance (QCM) can be applied to measure the exact density of the deposited coating but requires extra sample and experimental preparations. Therefore, approximate evaluation will be based on the available EDS spectrum studies which will be coupled with the results generated from Monte Carlo simulation of electron trajectory in solids (CASINO) to estimate average electron work volume with the exact energy used to study the spectrum [15]. This estimated work volume and cathodoluminescence is based upon the coating thickness but most importantly the density of the material. So, at a certain electron beam energy, a material which is not completely dense, will display substrate elemental peaks in

its energy spectrum, when compared to the same material, for the same thickness but it has a closer to theoretical density will not show substrate features in its energy spectrum.

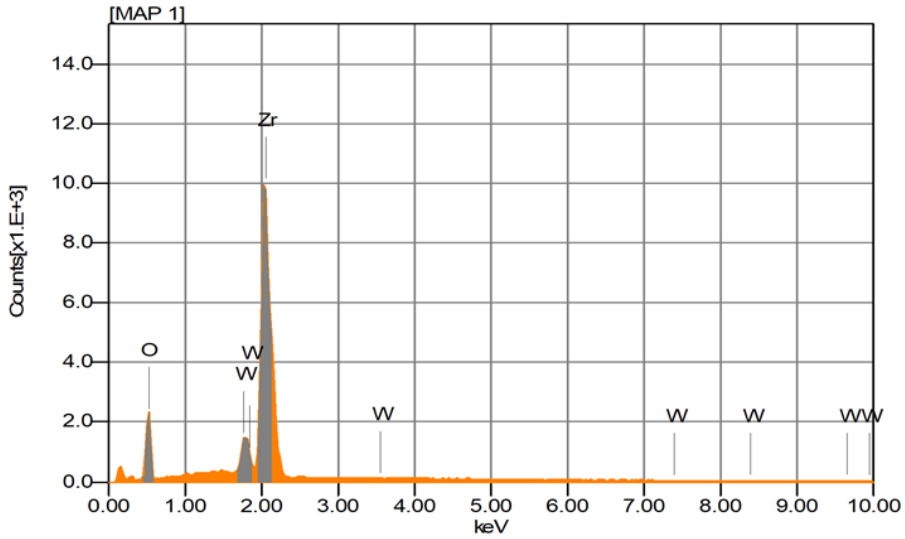

Figure 9: EDS spectrum performed with 15 KeV electron beams over the coated WC-Co surrogate particle with 1-micron ALD ZrO_2.

From step-by-step EDS spectrum studies performed with increasing electron beam energy (5 KeV to 15 KeV), it was determined that with 15 KeV beam, WC-Co elemental peak (W peak) is identified for the ALD ZrO_2 coating with ~1000 nm thickness (Figure 9). So, with the same electron beam energy in CASINO, it is simulated if that energy is enough to transmit through the thickness of the ZrO_2 coating which has the theoretical density (5.68 g/cc). Based on the result output shown in Figure 10 (a, b), it is not possible for the 15 KeV electrons to travel through and go to the surrogate material. The maximum depth the electrons can reach is ~ 800 nm (Figure 10 (a)). Therefore, it can be concluded that the deposited coating do not possess the theoretical density. Using the same CASINO model, different density values are tried that will fit the observed spectrum and show a small W peak. From iteration it was found the deposited coating will have a density of ~ 4.85 g/cc, because at this condition all the observed conditions are satisfied. Figure 11 (a, b) shows with 15 KeV electron beams, 1-micron ZrO_2 coating with density ~ 4.85 g/cc will result in W cathodoluminescence of ~ 0.7 % compared to 3.5% for Zr (so Zr CL % is 5 times, W). This is remarkably close to the peak ratios observed in the EDS spectrum where it is ~ 5.5 times.

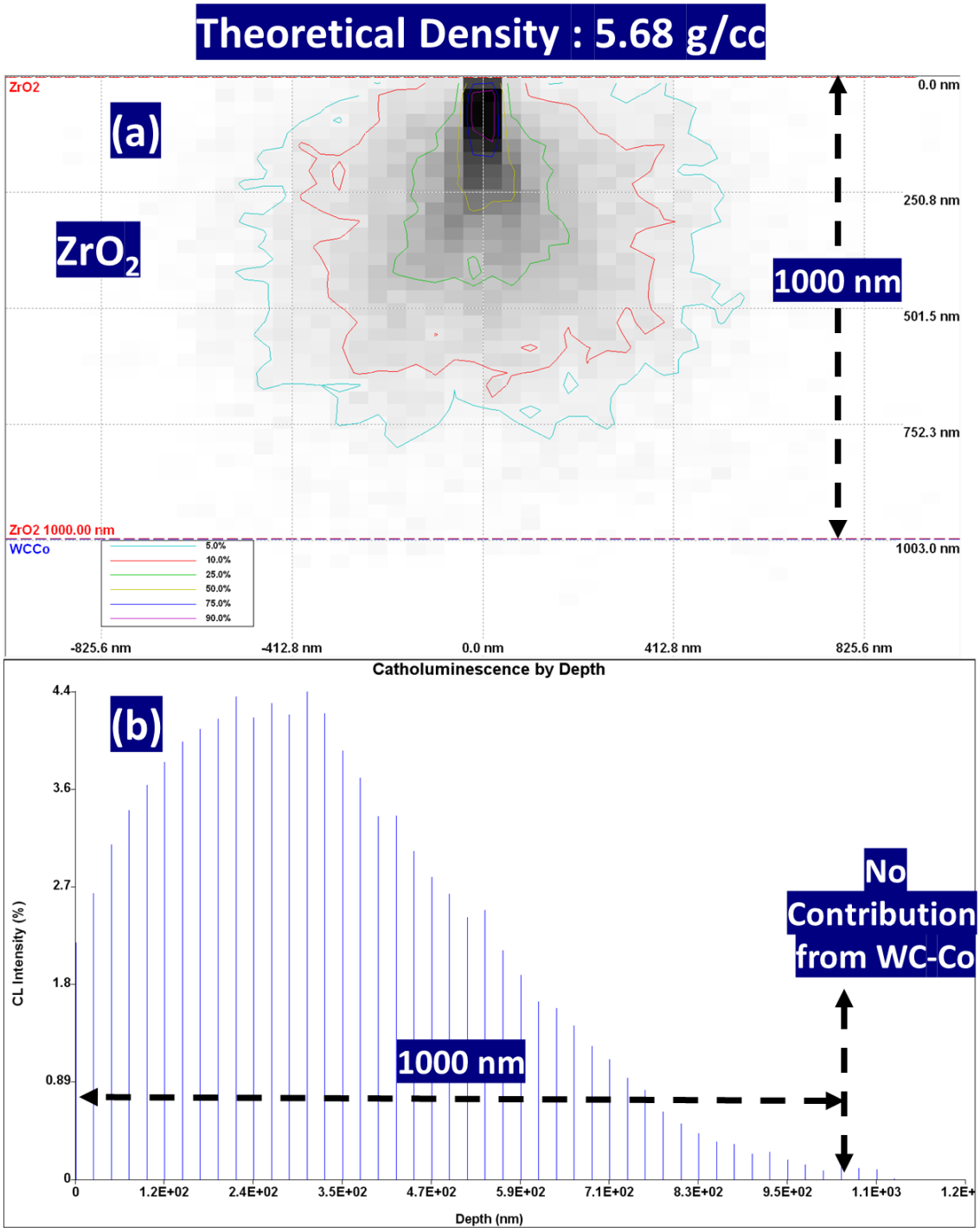

Figure 10: (a) CASINO based model result simulated with 15 keV e beam for a theoretically dense, 1-micron ZrO_2 coating (b) Cathodoluminescence result from the TD ZrO_2 coating, No contribution from WC-Co base is observed.

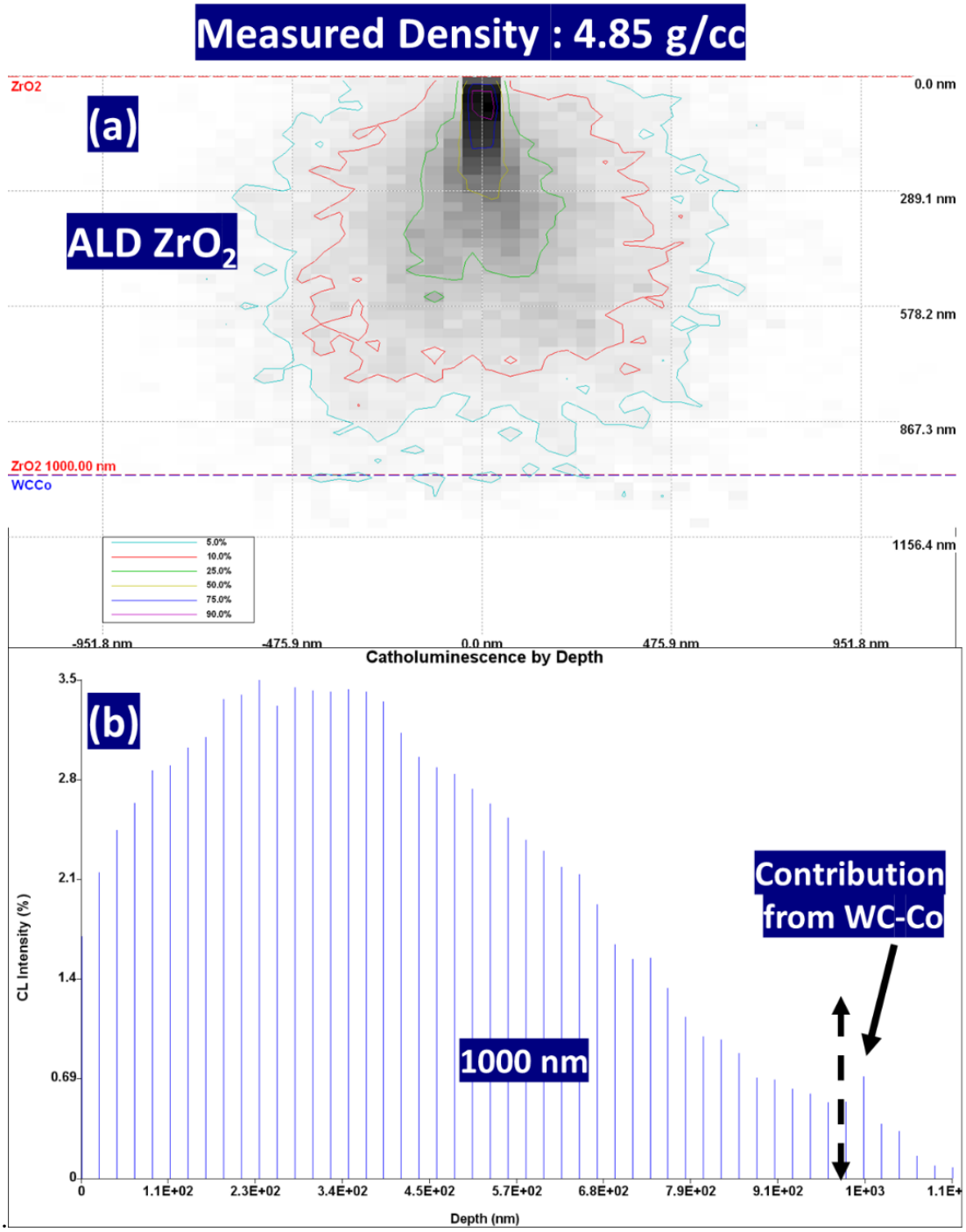

Figure 11: (a) CASINO based model result simulated with 15 keV e beam for 1-micron ZrO_2 coating with 4.85 g/cc density (b) Cathodoluminescence result from the TD ZrO_2 coating, some contribution from WC-Co base is observed.

4.2 Confirmation of ALD ZrN and ZrO_2 coating behavior over $UC_{1-x}N_x$ microspheres:

4.2.1 100 nm ALD ZrN over $UC_{1-x}N_x$ microspheres:

Based on the results developed from the WC-Co carbide micro-spheres, for ALD ZrN with 100 nm thickness, the process was transferred to the $UC_{1-x}N_x$ microspheres. Consistent with expectations, a remarkably similar result was observed from the coated fuel kernels as seen with the SEM, Figure 12 (a). No surface cracks, signs of spallation, or large cracks are observed. The EDS spectrum (Figure 12 (b)) also confirmed the same chemistry and chemical composition (Table 8) is developed during ALD ZrN growth over the fuel kernels.

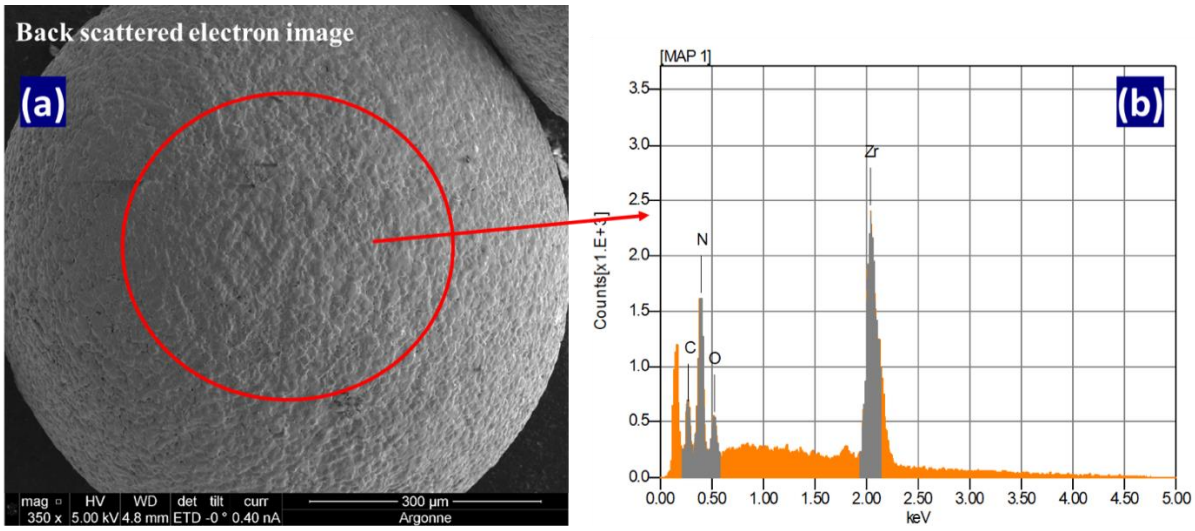

Figure 12: (a) SEM image of the as coated $UC_{1-x}N_x$ microspheres after applying 100 nm of ALD ZrN coating, (b) EDS spectrum from the region marked within red circle.

Table 8: $UC_{1-x}N_x$ microspheres surface composition after coated with 1000 cycles of ALD ZrN

Elements	mass%	Atom%
C	2.36	9.24
N	12.86	43.15
O	1.62	4.77
Zr	83.15	42.84

In order to measure the exact ZrN coating thickness achieved over the $UC_{1-x}N_x$ microspheres, FIB operation was done, where in total 5 coated surrogate particles were dug to expose a cross sectional region of ~ 40-micron x 30-micron. In each of those 5 dug particles, 10 different cross-sectional approximate measurements of the deposited coating were recorded. The mean thickness based on this measurement again came out to be ~ 110 nm (+/- 5 nm) of ALD ZrN after 1000 cycles of deposition, remarkably similar to the results studied for the surrogates. Figure 13 (a) is an example of one such area performed to expose the coating cross section. From Figure 13 (a), a continuous bonding between the ALD ZrN and $UC_{1-x}N_x$ microspheres is also observed.

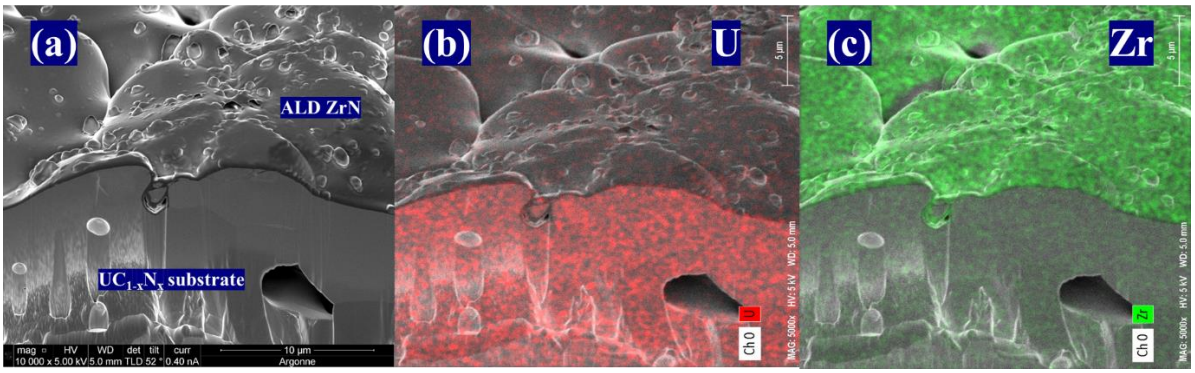

Figure 13: (a) FIB cross section of the ALD ZrN coating. From 10-point measurements, ~ 110 nm (+/- 5 nm) thickness was measured; (b) EDS mapping for U, (c) EDS mapping for Zr.

4.2.2 200 nm ALD ZrN over $UC_{1-x}N_x$ microspheres:

Based on the results developed from the WC-Co carbide micro-spheres, for ALD ZrN with 200 nm thickness, the process was transferred to the $UC_{1-x}N_x$ microspheres. Extremely simliar results were observed from the coated fuel kernels as seen with the SEM, presented in Figure 14 (a, b). As observed in the surrogate large surface cracks, significant signs of spallation are witnessed in the fuel kernel too. The EDS mapping (Figure 15 (a, b, c)) also confirmed the same observations as seen in Figure 14 (a, b). The deposited chemistry and chemical composition (Table 9) of the ALD ZrN over the fuel kernels are also similar to the measured values presented in Table 5 for the 200 nm coated surrogate material.

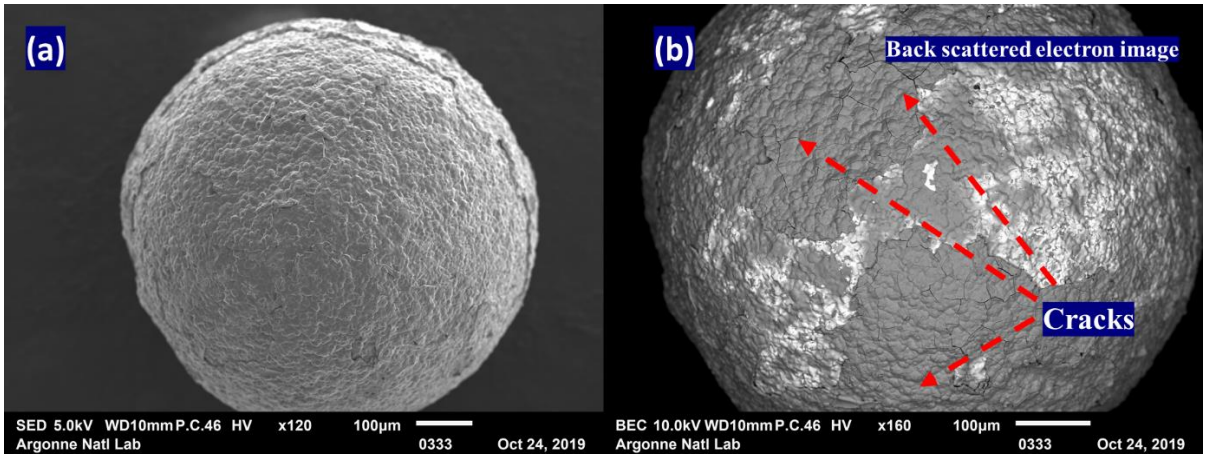

Figure 14: (a) SEM image of the as coated $UC_{1-x}N_x$ microspheres after applying 200 nm of ALD ZrN coating (b) Large cracks, spallation is observed all over the fuel kernel surface.

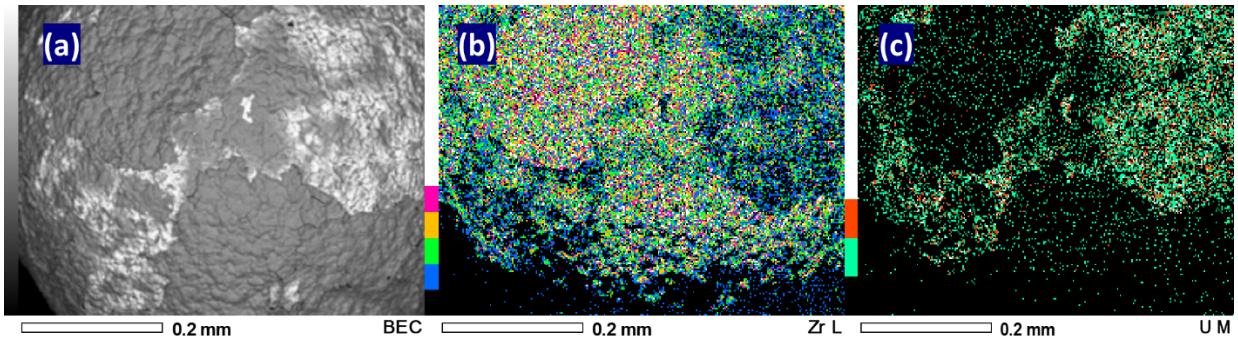

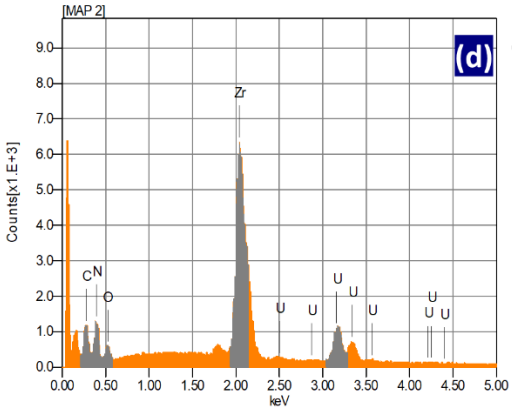

Table 9: $UC_{1-x}N_x$ microspheres surface composition after coated with 2000 cycles of ALD ZrN

Elements	Mass%	Atom%
C	2.43	16.78
N	5.01	29.66
O	0.96	4.98
Zr	29.68	26.99
U	61.92	21.58

Figure 15: (a) SEM image of the area selected over the $UC_{1-x}N_x$ microspheres coated with 2000 cycles of ALD ZrN, where the EDS mapping had been performed. (b) EDS mapping for Zr, (c) EDS mapping for U, (d) EDS spectrum from the mapped region. Table 9: Surface elemental composition of the mapped region.

4.2.3 1000 nm ALD ZrO_2 over $UC_{1-x}N_x$ microspheres:

Similar to the ALD ZrO_2 deposition over the surrogates, the ALD process with ZrO_2 coating was also transferred to the $UC_{1-x}N_x$ microspheres. Consistent with expectations, remarkably similar result was observed from the coated fuel kernels as seen with the SEM, Figure 16 (a). No surface cracks, signs of spallation, or large cracks are observed. The EDS spectrum (Figure 16 (b)) also confirmed the same elemental chemistry is developed during ALD ZrO_2 growth over the fuel kernels.

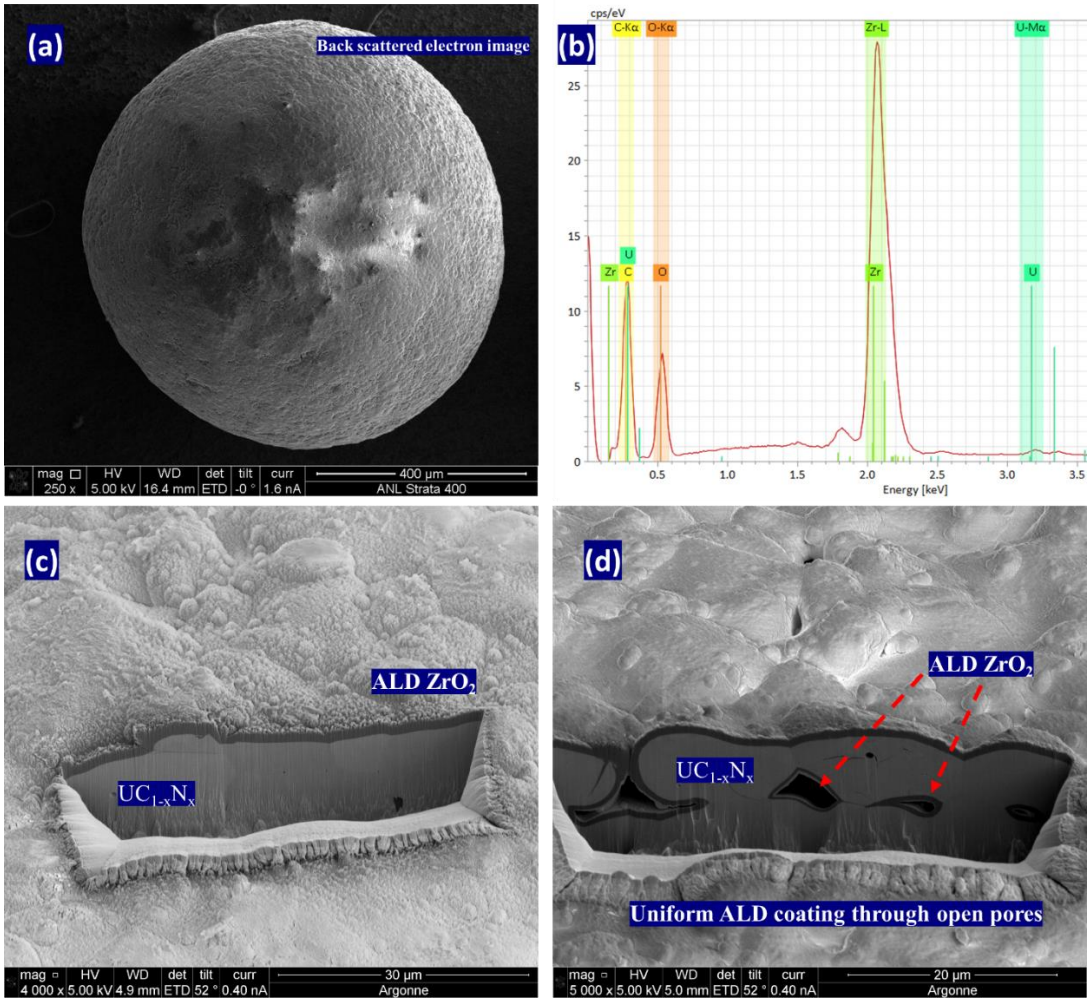

Figure 16: (a) FIB cross section of the ALD ZrN coating. From 10-point measurements, ~ 110 nm thickness was measured; The bright rectangular regions seen at the cross section is WC and the dark matrix is Co, (b) EDS Line scan performed at the cross section of the coated WC-Co particle, the red line over the line scan plot indicates interface between ZrN and WC-Co cemented carbide sphere.

To verify the coating thickness achieved over the $UC_{1-x}N_x$ microspheres with ALD ZrO_2, FIB operation was again done, where 5 coated surrogate particles were dug to expose a cross sectional region of ~ 40-micron x 30-micron. In each of those 5 dug particles, 10 different cross-sectional approximate measurements of the deposited coating were recorded. The mean thickness based on this measurement again came out to be ~ 1030 nm (+/- 100 nm) of ALD ZrN after 9100 cycles of deposition, remarkably similar to the results studied for the surrogates. Figure 16 (c) is an example of one such area performed to expose the coating cross section and 16 (d) displays the ability of ALD coating to infiltrate through open porous channels and deposit ultra-conformal coatings.

5 Future Work

More experiments and studies need to be done such that one micrometer (final target) of ALD ZrN coating development can be deposited over the $UC_{1-x}N_x$ microspheres without any issues of spallation and cracking. This may need solutions such as introduction of a compatible interlayer or even a multilayer solution where the coating design will consist ZrN/ZrO_2 (100 nm/5 nm) to achieve 1 micron. Even though 1-micron ALD ZrO_2 is successfully deposited over the fuel kernels, a great deal of material properties still need to be documented before the ALD ZrO_2 coating can be successfully used a high temperature diffusion barrier both against Zr and O_2. Experiments are needed to investigate things such as (a) whether the tetragonal crystal structure of the ALD ZrO_2 is stable when temperature variation is performed, (b) if it needs any second phase stabilizer to maintain the phase and prevent monoclinic transformation, (c) ZrO_2 stability under irradiation coupled with high temperature, and finally (d) the question of how ZrO_2 interacts with $UC_{1-x}N_x$ both under irradiation and at high temperature.

6 Conclusions

The execution and characterization of ALD coatings applied to surrogate materials yielded significant valuable information, and supported the development of Zr barrier coatings for uranium nitride fuel particles. Key conclusions from this work are as follows:

(1) Successful identification of ideal surrogate (WC-Co carbide composite) which can mimic $UC_{1-x}N_x$ microspheres mechanical and oxidation behaviors.

(2) Based on the ALD deposition over surrogates it is realized that no more than ~100 nm of ALD ZrN coating can be applied, as thicker coating leads to cracking and spallation, whereas 1-micron ALD ZrO_2 coating can successfully deposited without any issues.

(3) The deposited ALD ZrO_2 coating has a density of ~ 4.85 g/cc, compared to the theoretical density of 5.68 g/cc. This is ~ 86% of the TD.

(4) The deposition methods and the observed chemistry over the surrogates are completely transferrable and is verified from the similar observation done over $UC_{1-x}N_x$ fuel kernels.

Acknowledgement

This work was sponsored by the U.S. Department of Energy, Office of Nonproliferation Research and Development in the U.S. National Nuclear Security Administration Office of Defense Nuclear Nonproliferation under Contract DE-AC02-06CH11357.

References

[1] Alicia M. Raftery, Rachel Seibert, Daniel Brown, Michael Trammell, Andrew Nelson, and Kurt Terrani, "FABRICATION OF UN-MOCERMET NUCLEAR FUEL USING ADVANCED MANUFACTURING TECHNIQUES", Nuclear and Emerging Technologies for Space Knoxville, TN, 2020.

[2] Brian Jolly, Grant Helmreich, Kevin Cooley, John Dyer, Kurt Terrani, "FABRICATION AND CHARACTERIZATION OF SURROGATE TRISO PARTICLES USING 800μm ZrO2 KERNEL", ORNL/LTR-2016/315.

[3] R.W. Johnson, A. Hultquist, S.F. Bent, "A brief review of atomic layer deposition. from fundamentals to applications", Materials Today, 17 (2014), pp. 236-246.

[4] Galen R. Smolik, David A Petti, Stan T. Schuetz, "Oxidation, Volatilization, and redistribution of Molybdenum from TZM Alloy in Air", INEEL/EXT-99-01353.

[5] Martin Köppen, "Comparative Study of the Reactivity of the Tungsten Oxides WO2and WO3with Beryllium at Temperatures up to 1273 K", Condens. Matter 2019,4, 82.

[6] A.T. Nelson, E.S. Sooby, Y.-J. Kim, B. Cheng, S.A. Maloy, "High temperature oxidation of molybdenum in water vapor environments," Journal of Nuclear Materials, Volume 448, Issues 1–3, 2014.

[7] Fritsch website, https://www.fritsch-international.com/sample-preparation/milling/planetary-mills/details/product/pulverisette-7-premium-line/accessories/.

[8] S. Becker, E. Kim, R.G. Gordon, "Atomic Layer Deposition of Insulating Hafnium and Zirconium Nitrides", Chem. Mater., 16 (2004), pp. 3497-3501.

[9] Sumit Bhattacharya, Laura Jamison David, N. Seidman, Walid Mohamed, Y. Bei Michael, J. Pellin Abdellatif, M. Yacout, "Nanocrystalline ZrN thin film development via atomic layer deposition for U-Mo powder", J. of Nucl. Mat. 526 (2019) 151770.

[10] J.W. Elam, M. Schuisky, J.D. Ferguson, S.M. George, "Surface chemistry and film growth during TiN atomic layer deposition using TDMAT and NH_3", Thin Sol. Films, 436 (2003), pp. 145-156.

[11] Dennis M. Hausmann, Esther Kim, Jill Becker, and Roy G. Gordon, “Atomic Layer Deposition of Hafnium and Zirconium Oxides Using Metal Amide Precursors”, Chem. Mater.2002,14,4350-4358.

[12] Wenke Weinreicha, Lutz Wilde, Johannes Müller, and Jonas Sundqvist, “Structural properties of as deposited and annealed ZrO2 influenced by atomic layer deposition, substrate, and doping”, Journal of Vacuum Science & Technology A 31, 01A119 (2013),

[13 Sumit Bhattacharya, Kun Mo, Zhigang Mei, David Seidman, Bertrand Stepnik,
Michael J. Pellin, Abdellatif M.Yacout, “ Improving stability of ALD ZrN thin film coatings over U-Mo dispersion fuel”, Applied Surface Science, Volume 533, 15 December 2020, 147378.

[14] Wenke Weinreich, Lutz Wilde, Johannes Müller, and Jonas Sundqvist, “Structural properties of as deposited and annealed ZrO2 influenced by atomic layer deposition, substrate, and doping”, Journal of Vacuum Science & Technology A 31, 01A119 (2013).

[15] Drouin, D., Couture, A. R., Joly, D., Tastet, X., Aimez, V., & Gauvin, R. (2007). CASINO V2.42—A Fast and Easy-to-use Modeling Tool for Scanning Electron Microscopy and Microanalysis Users. Scanning, 29(3), 92–101. doi:10.1002/sca.20000.

Nuclear Science & Engineering Division
Argonne National Laboratory
9700 South Cass Avenue, Bldg. 208
Argonne, IL 60439

www.anl.gov

Argonne National Laboratory is a U.S. Department of Energy
laboratory managed by UChicago Argonne, LLC